

Neutron Diffraction Study of Field Cooling Effects on Relaxor Ferroelectrics Pb[(Zn₁₌₃Nb₂₌₃)_{0.92}Ti_{0.08}]₃O₃

Kenji Ohwada

Synchrotron Radiation Research Center (at SPRing-8),
Japan Atomic Energy Research Institute, 679-5148, Japan

Kazuma Hirota

Department of Physics, Tohoku University, Sendai 980-8578, Japan

Paul W. Rehrig^y

Materials Research Laboratory, The Pennsylvania State University, PA 16802, U.S.A.

Yasuhiko Fujii

Institute for Solid State Physics, The University of Tokyo, Kashiwa 277-8581, Japan

Gen Shirane

Department of Physics, Brookhaven National Laboratory, Upton, NY 11973-5000, U.S.A.

(Dated: April 14, 2024)

High-temperature (T) and high-electric-field (E) effects on Pb[(Zn₁₌₃Nb₂₌₃)_{0.92}Ti_{0.08}]₃O₃ (PZN-8%PT) were studied comprehensively by neutron diffraction in the ranges 300 < T < 550 K and 0 < E < 15 kV/cm. We have focused on how phase transitions depend on preceding thermal and electrical sequences. In the field cooling process (FC, E k [001] = 0.5 kV/cm), a successive cubic (C) → tetragonal (T) → monoclinic (M_C) transition was observed. In the zero-field cooling process (ZFC), however, we have found that the system does not transform to the rhombohedral (R) phase as widely believed, but to a new, unidentified phase, which we call X. X gives a Bragg peak profile similar to that expected for R, but the c-axis is always slightly shorter than the a-axis. As for field effects on the X phase, we found an irreversible X → M_C transition via another monoclinic phase (M_A) as expected from a previous report [Noheda et al. Phys. Rev. Lett. 86, 3891 (2001)]. At a higher electric field, we confirmed a c-axis jump associated with the field-induced M_C → T transition, which was observed by strain and x-ray diffraction measurements.

PACS numbers: 61.12.-q, 77.65.-j, 77.84.Dy

I. INTRODUCTION

Solid solutions of Pb(Zn₁₌₃Nb₂₌₃)O₃ and PbTiO₃ (PZN-xPT) are relaxor ferroelectrics with extremely high piezoelectric responses [1, 2], which are an order of magnitude larger than those of conventional piezoelectric ceramics such as Pb(Zr_xTi_{1-x})O₃ (PZT) [3, 4]. PZN-xPT has a cubic (C) perovskite-type structure at high temperatures, and undergoes a diffuse ferroelectric phase transition at low temperatures. It has been reported that the ferroelectric region is separated into rhombohedral (R) and tetragonal (T) symmetries by a morphotropic phase boundary (MPB), a nearly vertical line between the two phases, at x ≈ 10%. The piezoelectric response of PZN-xPT reaches the maximum at x = 8%, which is located on the R (lower x) side near MPB [1]. These behaviors are qualitatively similar to those of PZT. However, PZN-

xPT can be grown in single crystal form unlike PZT, so that the structural properties can be studied in more detail.

A typical strain-field loop for a poled PZN-8%PT single crystal at room temperature (RT), where an electric field is applied along the pseudo-cubic [001] direction (E k [001]), is shown in Fig. 1(a) after Park and Shrout. The strain increases linearly below a certain threshold field, then jumps discontinuously, which is called the c-jump. Durbin et al. studied PZN-8%PT by x-ray diffraction and found that the field dependence of the lattice parameter exactly reflects the strain behavior, which indicates the observed high macroscopic strain levels indeed originate from the microscopic strain of the lattice [5]. In addition, they found that the structure of PZN-8%PT exhibits an irreversible change from the zero-field R phase to different phases by applying electric fields [6]. Subsequent x-ray measurements at RT by Noheda et al. have identified the symmetries of the various phases appearing in PZN-8%PT [7, 8]. They have shown that the zero-field R phase starts to follow the direct polarization path to the T symmetry via an intermediate monoclinic (M_A) phase [9], but then jumps irreversibly to an alternate path involving a different type of monoclinic distortion

Electronic address: ohwada@spring8.or.jp

^yPresent address: TRS Ceramics, Inc., 2820 East College Ave.
State College, PA 16801, U.S.A.

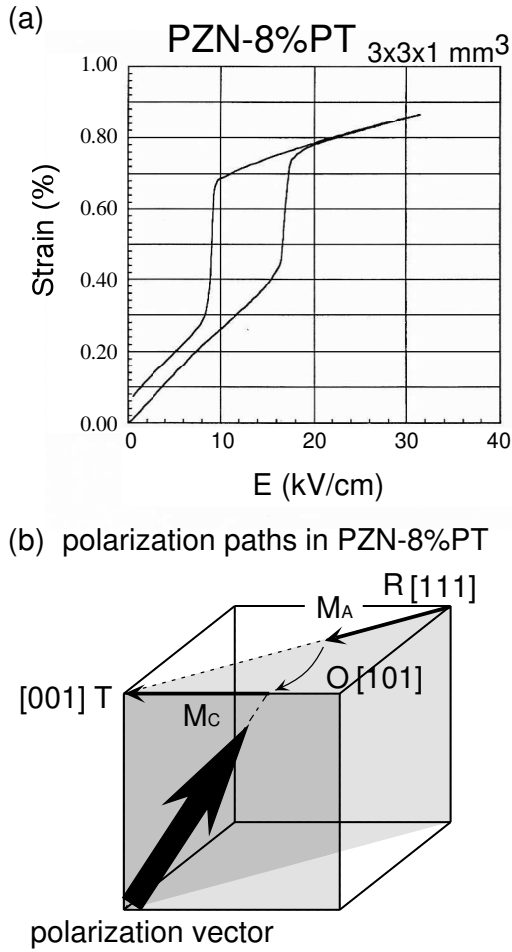


FIG. 1: (a) Electric field dependence of the strain measured for the $3 \times 3 \times 1 \text{ mm}^3$ PZN-8%PT crystal. (b) Polarization rotation path for the PZN-8%PT crystal ($R \rightarrow M_A \rightarrow M_C \rightarrow T$).

(M_C) [9], as schematically drawn in Fig. 1 (b). Their result suggests that there is a very narrow region of monoclinic phase nestled against MPB as found for PZT.

The maximum piezoelectric activity is located in the monoclinic phase near MPB in both PZT and PZN-xPT. These observations have resulted in the concept of the polarization rotation mechanism by Fu and Cohen [10], which successfully explains the ultra-high electromechanical response. Whereas the direction of the polarization vector in a conventional tetragonal ferroelectric phase is fixed to the [001] (e.g., PbTiO₃) or [111] (e.g., BaTiO₃) direction, the monoclinic symmetry allows the polarization vector a much greater degree of freedom as it is only constrained to lie within the (110) plane for M_A and the (010) plane for M_C . In the monoclinic phases, the polarization direction can easily adjust to the electric field, thus naturally gives a large piezoelectric response. Although the presence of a monoclinic phase in a cubic perovskite system seems quite unusual, it is now understood within the framework of an extended Devonshire

theory for strongly anharmonic crystals, which require higher order terms [11].

As described above, PZN-8%PT shows a complicated field-induced phase transitions: $R \rightarrow M_A \rightarrow M_C \rightarrow T$ on increasing field and $T \rightarrow M_C$ on decreasing field [7, 8]. To clarify the origin of the exceptional piezoelectric character of this system, it is necessary to resolve the complexities of the transformation sequences in more detail. Ohwada et al. have carried out neutron diffraction experiments on PZN-8%PT single crystals as a function of applied electric field [12]. They have confirmed the irreversible $R \rightarrow M_A \rightarrow M_C$ sequence reported in x-ray diffraction experiments. However, the sharp c-jump observed in strain and x-ray measurements was not reproduced. Instead, they have found a marked asymmetry of the (002) Bragg peak line shapes along the c-axis, indicating a non-uniform strain distribution within the crystal, which washes out the c-jump. Their subsequent high-energy x-ray study of the same crystals has supported this view.

In the present study, we have carried out high-q-resolution neutron diffraction experiments of PZN-8%PT in the temperature and electric field ranges 300–550 K and 0–15 kV/cm, which are significantly extended than those of the previous work. We have particularly focused upon how phase transitions depend on preceding thermal and electrical sequences. The present article is organized as follows: The experimental details are given in Section II. In Section III, we show our experimental results on the structural phase transitions under various sequences. We first clarify that PZN-8%PT does not transform to the R phase in the zero-field cooling (ZFC) process as widely believed, but to a yet unidentified phase, which we call the X phase. We then describe the temperature dependence in the field cooling (FC) process, and the electric field dependence at fixed temperatures. These results are summarized in an E-T phase diagram. Discussions on the novel X phase and the established E-T phase diagram are given in Section IV.

II. EXPERIMENTAL DETAILS

Neutron diffraction measurements have been performed mainly on the $8 \times 8 \times 2 \text{ mm}^3$ single crystal. This crystal was grown by the flux solution method [13] at the Pennsylvania State University. The as-grown crystal was poled at 10 kV/cm at RT. The strain curves measured along [001] as a function of electric field were used to check the quality of the crystals. As shown for a typical example in Fig. 1, the crystals we studied exhibit a sharp jump in the c-axis lattice spacing around 15 kV/cm.

The neutron diffraction experiments were carried out on the Tohoku University triple-axis spectrometer TOPAN (6G) installed in the JRR-3M reactor located at the Japan Atomic Energy Research Institute in Tokai, Japan. Most of the experiments were performed using the tight horizontal beam collimation $15^\circ\text{-}10^\circ\text{-}5^\circ\text{-}10^\circ\text{-}B$ (S

= Sample, B = Blank) with two pyrolytic graphite (PG)

filters before and after the sample to eliminate higher harmonics in the neutron beam. The incident neutron energy (E_i) was tuned to 14.7 meV ($\lambda = 2.36 \text{ \AA}$) with a highly oriented PG (HOPG) monochromator. Gold electric wires insulated with alumina tubes were carefully connected to the sample which was mounted on the cold head of a high-temperature closed cycle refrigerator (HT-CTL, 15 T 600 K). A high electric field was generated with the MATSUSADA AR-series high voltage power supply. The sample was wrapped with the glass wool for electric insulation, and fixed softly to a specially designed copper sample holder with care not to give unnecessary stress.

The crystal was oriented to give the (HOL) scattering plane and the electrodes were attached to the (001) surfaces. Thus electric field was applied along the pseudocubic [001] direction in the present study. The lattice constant of PZN-8%PT in the cubic phase at $T = 540 \text{ K}$, $E = 0 \text{ kV/cm}$ is $a = 4.04 \text{ \AA}$, thus the 1 r.l.u. [14] corresponds to $a (= b) = 2/a = 1.555 \text{ \AA}^{-1}$. We used the $a (= b)$ value at 1.555 \AA^{-1} all the time for reciprocal lattice scanning. Scans were carried out immediately after changing the sample condition.

III. PHASE TRANSITIONS

First of all, we show the Electric field-Temperature (E - T) phase diagram of PZN-8%PT in Fig. 2 which summarizes our present structural measurements. Circles represent the transition temperatures and fields which were determined by changes of the lattice constants and peak profiles. An arrow indicates the scanning direction and range of the corresponding measurement sequence.

A. X phase

We studied the temperature dependence of the lattice constants of PZN-8%PT crystal under zero electric field (ZF, $E = 0.0 \text{ kV/cm}$). The sample was firstly heated up to 560 K, where we confirmed the symmetry is cubic. At 500 K in the ZFC process, the PZN-8%PT crystal transforms into the T phase from the C phase as expected, associated with 90° domain formation, which was confirmed by observing a peak splitting of the (002) reflection along the [001] direction. By fitting the (002) reflection with a double Gaussian function, we obtained the temperature dependence of the lattice constants c_T and a_T as shown in Fig. 3.

To confirm the T to R phase transition, we cooled down the sample further. Quite unexpectedly, however, we have found that the system does not transform into the R phase at 340 K on cooling as widely believed so far, but to an unidentified phase. We will call it the X phase in the present article. Figure 4 shows the (200) and (002) peak profiles in the C and X phases. The (200) and (002)

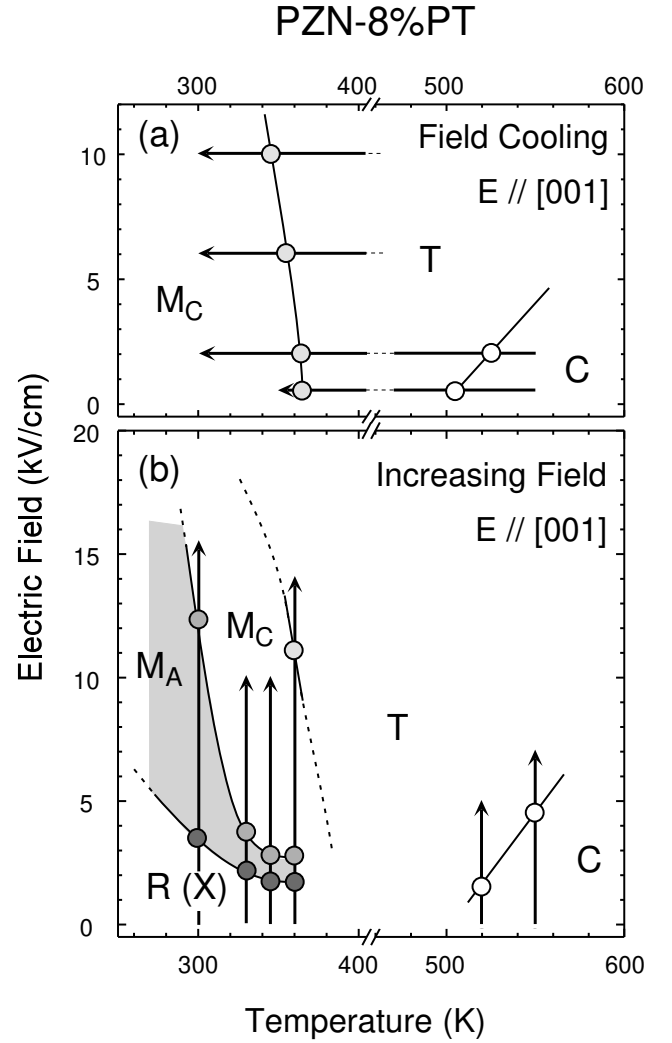


FIG. 2: E - T phase diagram of PZN-8%PT. (a) is obtained from structural measurements in the FC process. (b) is obtained from the increasing electric field process after ZFC (and ZFH for the X phase). Arrows indicate the scanning directions and ranges of the corresponding measurement sequences. Circles represent the transition temperatures and fields determined from each sequence.

peak profiles are perfectly centered when a and b were set to the same value (1.555 \AA^{-1} in the C phase). On the other hand, the peak center of the (002) profiles in the X phase shifts to higher q compared with that of (200), which indicates PZN-8%PT is not in the R symmetry after ZFC. We also studied (101) peak profile and found no sign of the expected peak split of the rhombohedral structure, although a mosaic broadening was observed. As for the lattice constants, c_T gradually increases with decreasing temperature and suddenly drops with a large amount at 340 K, where the T \rightarrow X phase transition takes place.

Although it is not shown in Fig. 3, we also observed the intensity jump at the transition temperatures, 500 K and

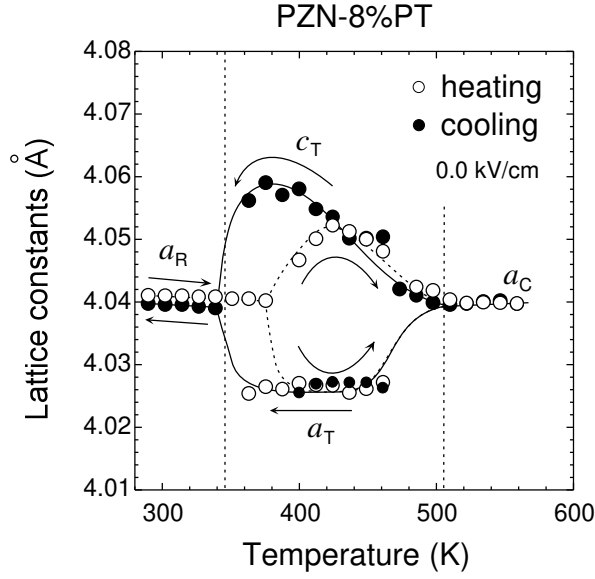


FIG. 3: Temperature dependence of the lattice constants under zero electric field $E = 0.0$ kV/cm by monitoring the (002) reflection. C \rightarrow T \rightarrow X transition sequence is clearly seen.

340 K. The integrated intensity of the (002) reflection in the X phase (I_X) is 1.5 times larger than that in the T-phase (I_T), and five times larger than that in the C-phase (I_C) ($I_X : I_T : I_C = 5 : 3 : 1$), which indicates that the extinction effect [15] is phased out through transitions. In the zero-field heating process (ZFH), the X \rightarrow T phase transition takes place at 380 K with a large hysteresis; the transition temperature is 40 K higher than that of the cooling process, while the T \rightarrow C phase transition shows a small hysteresis ~ 10 K.

B. Temperature dependence of lattice constants in FC process

To clarify the electric field effects on the phase transition sequence as represented in Fig. 2(a), we studied the temperature dependence of the lattice constants of PZN-8%PT crystal under fields ($E = 0.5, 2.0, 6.0, 10.0$ kV/cm) on cooling, thus FC processes. To obtain a comprehensive picture of the PZN-8%PT structural properties under the FC process, we took mesh scans around the (002) and (200) reflections at 540 K, 400 K and 300 K with the electric field $E = 0.5$ kV/cm (see Fig. 5). As mentioned in Section II, we fixed the a and b values at 1.555 \AA^{-1} throughout the scans. The followings are remarks of the mesh scan results. (a) At 540 K, neither elongation nor contraction of the lattice constants was seen. The PZN-8%PT system is still in the cubic symmetry. (b) At 400 K, the elongation of the lattice constant c_T and the contraction of the lattice constant a_T were clearly seen. Thus the PZN-8%PT crystal trans-

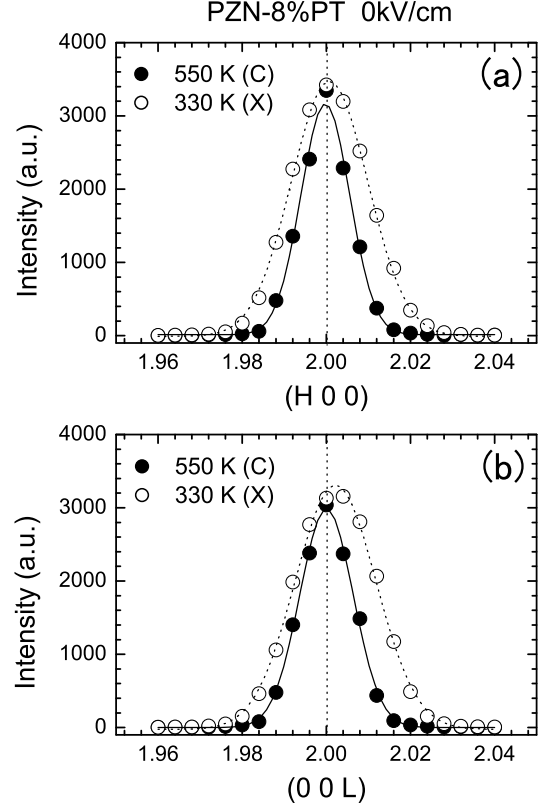


FIG. 4: The (H 0 0) and (0 0 L) peak profiles of the C phase and X phase respectively. Solid and dotted lines drawn through the data points are for guides to the eyes.

forms into the T phase. As shown in the contour maps of Fig. 5, additional peaks appear near (002) and (200) in the T phase. These peaks indicate a 90° domain formation along the fl_01g pseudo-cubic plane [16]. (c) The M_C phase appears. As shown in Fig. 5(c), the (200) peak split into three peaks i.e. (200) twin peaks and one (020) single peak, while the (002) peak remains as a single peak.

Figure 6 shows the temperature dependence of the lattice constants observed at $E = 2.0$ kV/cm. We also measured the (200) reflection at 450 K, the (200) and the (020) reflections at 300 K to obtain the information of the lattice constant a_T at 450 K, a_{M_C} and b_{M_C} at 300 K respectively. The lattice constant c_T gradually increases as the temperature decreases and suddenly drops largely at 340 K, where the T \rightarrow M_C phase transition takes place.

C. Electric field dependence of lattice constants at fixed temperatures

To construct Fig. 2(b), we also observed the electric field (E) dependence of the lattice constants at some selected temperatures: (1) From the C phase at 550 K and

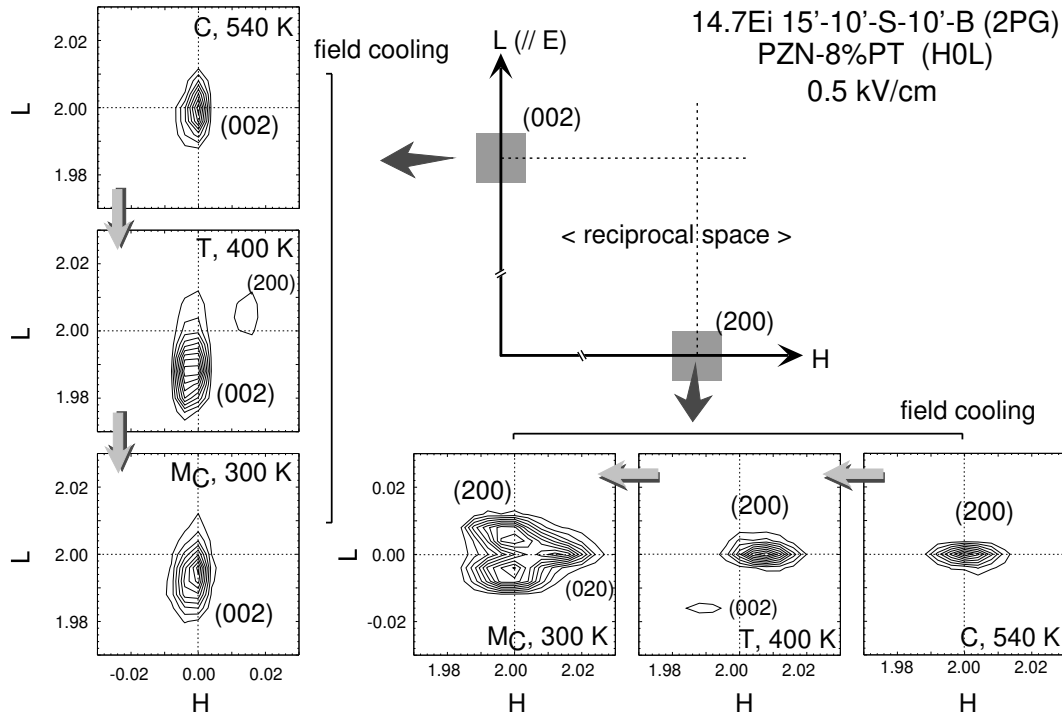


FIG. 5: Mesh scans around the (002) and (200) at 540 K under the zero-electric field $E = 0.0$ kV/cm and at 400 K and 300 K under $E = 0.5$ kV/cm.

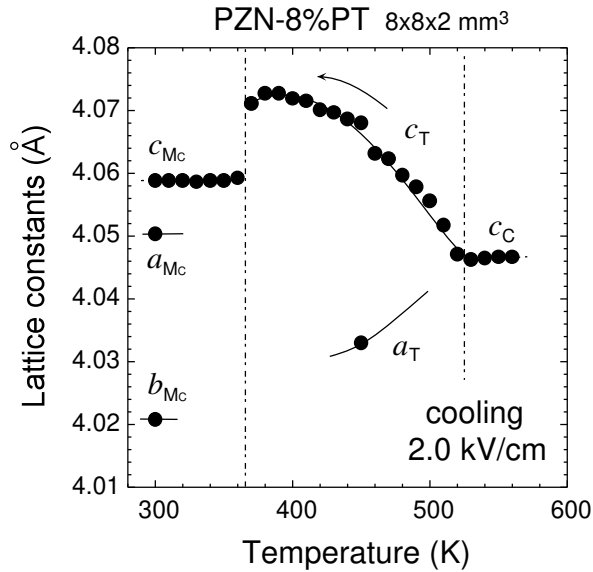


FIG. 6: Temperature dependence of the lattice constants under the electric field $E = 2.0$ kV/cm. The M_C phase is stable at RT in contrast to the ZF cooling result. Solid lines drawn through the data points are for guides to the eyes.

520 K, (2) From the X phase at 300 K, 330 K, 345 K, and 360 K. The X phase in (2) was realized by FC from 550 K to 300 K followed by FH to the target temperature.

Note in particular that PZN-8%PT is in the $T \rightarrow X$ hysteresis loop at 360 K. Following the precedent routine, we also took a (HOL) mesh scan around the pseudo-cubic (200) position. As mentioned before, the peak structure around (200) strongly depends on the nature of the phase appearing in PZN-8%PT. Figure 7 shows the electric field dependence obtained at a fixed temperature of 345 K. We observed the irreversible $X \rightarrow M_A \rightarrow M_C$ transition sequence which was found out by Noheda et al. [7, 8, 12]. The M_A phase is stable at room temperature for more than two weeks after the field removal, and shows no relaxation of the crystal lattice.

Figure 8 shows the electric field dependence of (a) the lattice constants and (b) the θ_{90} value, observed at 330 K. a_X and c_X show no field dependence. Above $E = 2.0$ kV/cm, on the other hand, PZN-8%PT transforms into the M_A phase with a large elongation of a_{M_A} and shrink of a_{M_C} [17]. A peak split suddenly takes place at 2.0 kV/cm and θ_{90} [18] shows a gradual increment as the field increases. The M_A phase exists only in the range $2.0 \leq E < 3.5$ kV/cm, which is shown by gray region in Fig. 8. The width of the omega scan [19], which corresponds to the crystal mosaic width, is also drastically changed from ~ 0.2 to ~ 0.1 within the M_A phase as the field increases. The field dependent behavior of the lattice constants a_{M_A} and the a_{M_C} observed in the field range $2.0 \leq E < 3.5$ kV/cm seemed to be non-linear to the electric field, which is usually seen in the domain rotation properties by the bulk measurements [20]. Since

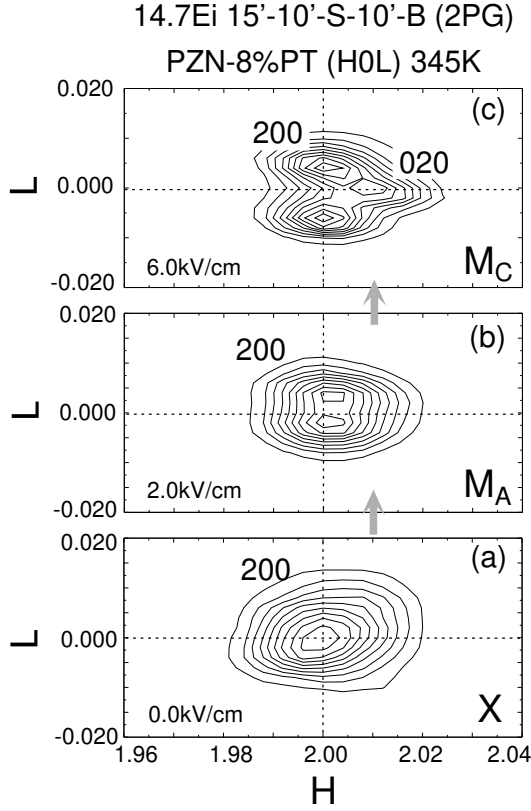


FIG. 7: Electric field dependence of the (H0L) contour around the pseudo-cubic (200) obtained at 345 K.

we observed the lattice constants, this anomalous property of the lattice constants does not originate from the macroscopic domain rotation.

Above 3.5 kV/cm, the M_A phase transforms into the M_C phase with a gradual change in spite of the polarization jump from the intrapseudo-cubic $f\bar{1}\bar{1}0g$ plane to intrapseudo-cubic $f010g$ plane (see Fig. 1(b)). Up to 10 kV/cm, the lattice constant c_{M_C} elongates and the b_{M_C} shrinks continuously. On the other hand, the lattice constant a_{M_C} does not show the field dependence. The

$\beta_{90.0}$ value also represents a gradual increment up to 10 kV/cm. After removing the field, the lattice constants do not return to the home position, but still remain in the M_C symmetry. It is now clear that the M_C phase is another ground state of PZN-8%PT at 330 K.

Next we measured the c -axis jump (c -jump) on the poled PZN-8%PT crystal at 360 K which is located inside the hysteresis loop of the reversible $T \rightarrow M_C$ phase transition. A sharp c -jump was clearly seen by strain and x-ray measurements at room temperature at high electric field 15 kV/cm as shown in Fig. 1(a). As mentioned before, Noheda et al. clarified using high energy x-rays that the crystal surface behaves differently from the crystal bulk at RT [8], i.e. the field inducing the $M_C \rightarrow T$ transition is 7 kV/cm for the bulk and 20 kV/cm for the near surface region [8]. Neutrons easily penetrate

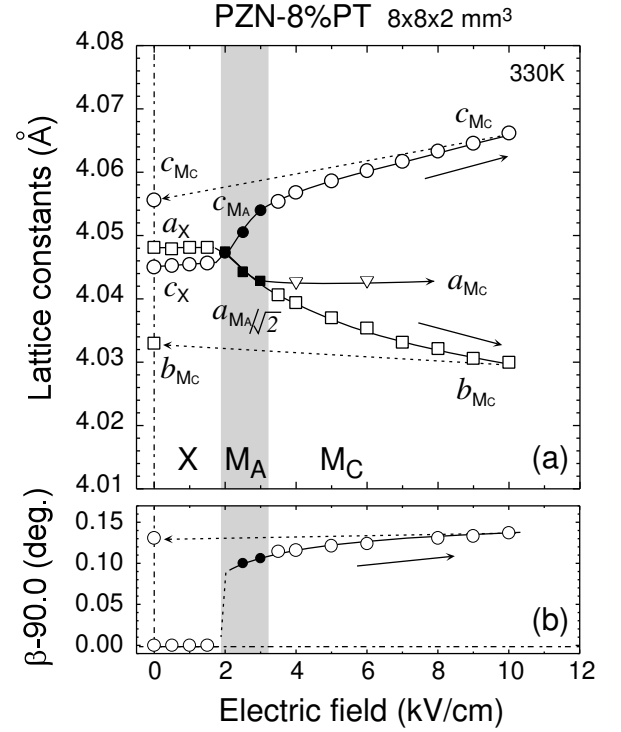


FIG. 8: Electric field dependence of (a) the lattice constants and (b) $\beta_{90.0}$ observed at 330 K. Solid lines drawn through the data points are for guides to the eyes.

a crystal and give us the bulk information more than any other measurements. Figure 9 shows the hysteresis loop of the c lattice constant, which represents the field induced $M_C \rightarrow T$ phase transition of PZN-8%PT. The c_{M_C} gradually increases non-linearly and shows a small jump, which is contrary to the one as seen in Fig. 1(a). This is ascribed to a strain distribution in the bulk [12].

IV. DISCUSSIONS

A. X phase

Let us first discuss the X phase introduced in Section III. As shown in Fig. 8(a), the lattice constants a_X and c_X at $E = 0.0$ kV/cm show a significant difference as much as 0.07%. This difference is also seen in the (200) and (002) peak profiles of the C phase and X phase as depicted in Fig. 4. This means that the PZN-8%PT crystal is not in the Rhombohedral symmetry after the ZFC process as it has been long believed. An important question is how PZN-8%PT can distinguish between the a_X and c_X directions under the ZFC process. This is most likely due to a sample treatment effect such as poling, quenching, attachment of electrodes to the c plane, sample holding and so on. It would be interesting to study the effects on the X phase formation.

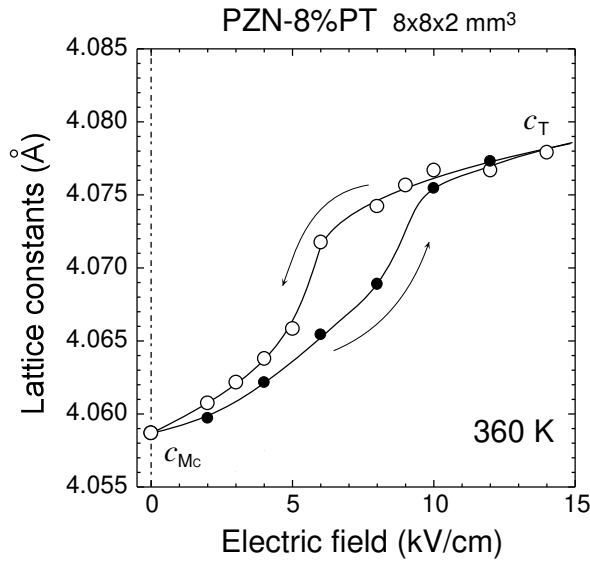


FIG. 9: A hysteresis loop of the lattice constant c representing the $M_C \rightarrow T$ phase transition of PZN-8%PT. Solid lines drawn through the data points are for a guide to the eyes.

As for the microscopic mechanism, a phase shift model proposed by Hirota et al. [21] for the relaxor $\text{PbMg}_{1/3}\text{Nb}_{2/3}\text{O}_3$ (PMN) would give a clue to understand the X phase. They analyzed the diffuse intensity of PMN and found that the ionic displacements are divided into two categories; a phase shift (shift) common to all the ions and each ionic displacement which satisfies the center of mass condition as is the case for ordinary ferroelectric systems such as PbTiO_3 . It is speculated that the inhomogeneity of Mg^{2+} and Nb^{5+} distribution creates a local electric field gradient and interacts with Polar N and R regions resulting in such a phase shift. If the Mg^{2+} and Nb^{5+} distribution orients to a certain direction by a sample treatment as presented above, the phase shift is also oriented and results in the anisotropy of the crystal lattice. We speculate that this type of phase shift also exists in the PZN-8%PT crystal and causes a significant difference between the a_x and c_x lattice constants.

One of the main goal for the relaxor physics is to understand and calculate how a large piezoelectric response is realized. The discovery of the novel X phase as a ground state of PZN-8%PT around RT urges revisions of theoretical frameworks of relaxors. In particular, the polarization rotation mechanism [10], which successfully explains the high electromechanical responses, is largely based on the correct assignment of the symmetries of various structural phases. It is thus very important to identify the space group of the X phase.

B. E-T phase diagram

As described in Section III, we have constructed the E-T phase diagram of PZN-8%PT. Figure 2(a) summarizes the results obtained in the FC process. The $C \rightarrow T$ phase boundary shifts to higher temperature and the $T \rightarrow M_C$ phase boundary shifts slightly to lower temperature as the field increases, which indicates that the T phase is stabilized under a high electric field. The M_A phase never appears in the FC process even when the field is very low, as experimentally confirmed down to $E = 0.5$ (kV/cm). Although it is not shown in Fig. 2(a), the M_C phase is stable even at 15 K. Figure 2(b) summarizes the field increasing process at a fixed temperature after ZFC (and ZFH for X phase). At high temperature, the C phase transforms into the T phase reversibly and the phase boundary shows the same feature as that in Fig. 2(a). At low temperature, the X phase irreversibly transforms into the M_A phase at a lower field. The M_A phase is represented by the gray region in Fig. 2(b). Note that the X and M_A phases become stable as the temperature decreases. As already stated above, the M_A phase does not relax at least for two weeks. The PZN-8%PT crystal further transforms into the M_C phase at a higher field irreversibly. Once the M_C phase is obtained (PZN-8%PT poled crystal), the X and M_A phases no longer recover. Only the reversible $M_C \leftrightarrow T$ phase transition takes place at higher field as seen in the strain-field (Fig. 1(a)) and x-ray measurements.

It has been reported that the PZN-9%PT crystal has the orthorhombic (O) symmetry at RT after applying field [22]. Let us consider a new phase diagram which has the composition (x) axis perpendicular to the E-T plane. In that phase diagram, it is clear that the O phase is indeed very close to the M_C phase. We speculate that a hidden O symmetry exists in the PZN-8%PT at RT and gives birth to the M_C symmetry, which polarization is located on the $T \rightarrow M_C \rightarrow O$ polarization rotation path as shown in Fig. 1(b). Park et al. reported that, in the PZN-xPT system, the M_C symmetry near MPB gives a higher piezoelectricity than the M_A symmetry (lower x) does [1]. This difference can be ascribed to the background symmetry of each phase: the O symmetry for M_C and the R symmetry for M_A . The O symmetry requires the [001] electric field much higher than that for the R symmetry, resulting in the higher piezoelectricity of the M_C phase.

V. SUMMARY

We made comprehensive neutron-diffraction studies on high-temperature and high-electric-field effects on $\text{Pb}[(\text{Zn}_{1/3}\text{Nb}_{2/3})_{0.92}\text{Ti}_{0.08}\text{O}_3]$ (PZN-8%PT) in the ranges 300–550 K and 0–15 kV/cm. In the field-cooling process (FC, $E = 0.5$ kV/cm), a successive cubic (C) \rightarrow tetragonal (T) \rightarrow monoclinic (M_C) transition was observed. In the zero-field-cooling process (ZFC),

however, we have found that the system does not transform to the rhombohedral (R) phase as widely believed, but to a new, unidentified phase, which we call X. X gives a Bragg peak profile similar to that expected for R, but the c-axis is always slightly shorter than the a-axis. We expect that the discovery of the novel X phase as a ground state of PZN-8% PT urges revisions of theoretical frameworks of relaxors. As for field effects on the X phase, we found an irreversible $X \rightarrow M_C$ transition via another monoclinic phase (M_A) as expected from a previous report [7]. At a higher electric field, we confirmed a c-axis jump associated with the field-induced $M_C \rightarrow T$ transition, as observed by strain and x-ray diffraction measurements. Our precise E-T phase diagram will provide a fundamental aspect for future studies of relaxors. Our next goal is to clarify a true character of the X phase.

After this work was completed, we have learned that a novel phase, which is similar to the X phase of PZN-

8% PT, was found in PZN at room temperature by high energy x-ray diffraction [23].

Acknowledgments

We would like to thank P.M. Gehring, S-E. Park, B. Noheda and S. Wakimoto for stimulating discussions, as well as Y. Kawamura for technical support. We are also grateful to G. Xu and his collaborators for informing us of their high energy x-ray results on PZN prior to publication. This work was supported by U.S.-Japan Cooperative Research Program on Neutron Scattering between the U.S. Department of Energy (USDOE) and the Japanese MONBU-KAGAKUSHO. We also acknowledge financial support from the USDOE under Construction No. DE-AC02-98CH10886.

-
- [1] S-E. Park, and T. R. Shrout, J. Appl. Phys. 82, 1804 (1997).
 - [2] S.F. Liu, S-E. Park, T. R. Shrout and L. E. Cross, J. Appl. Phys. 85, 2810 (1999).
 - [3] J. Kuwata, K. Uchino, and S. Nomura, Ferroelectrics, 37, 579 (1981).
 - [4] J. Kuwata, K. Uchino, and S. Nomura, Jpn. J. Appl. Phys. 21, 1298 (1982).
 - [5] M. K. Durbin, E.W. Jacobs, J.C. Hicks, and S-E. Park, Appl. Phys. Lett. 74, 2848 (1999).
 - [6] M. K. Durbin, J.C. Hicks, S-E. Park, and T. R. Shrout, Appl. Phys. 87, 8159 (2000).
 - [7] B. Noheda, D. E. Cox, G. Shirane, S-E. Park, L. E. Cross and Z. Zhong, Phys. Rev. Lett. 86, 3891 (2001).
 - [8] B. Noheda, Z. Zhong, D. E. Cox, G. Shirane, S-E. Park and P. Rehrig, Phys. Rev. B 65, 224101 (2002).
 - [9] The polarization vectors lie in the pseudo-cubic $f\bar{1}0g$ ($f10g$, $f010g$) plane in M_A (M_B , M_C). This notation is proposed by Vanderbilt and Cohen [11].
 - [10] H. Fu and R. Cohen, Nature 403, 281 (2000).
 - [11] D. Vanderbilt and M. H. Cohen, Phys. Rev. B 63, 094108 (2001).
 - [12] K. Ohwada, K. Hirota, P.W. Rehrig, B. Noheda, Y. Fujii, S-E. Park and G. Shirane, J. Phys. Soc. Jpn. 70, 2778 (2001).
 - [13] M-L. Mulvihill, S-E. Park, G. Risch, Z. Li, K. Uchino, T-R. Shrout, Jpn. J. Appl. Phys. 35, 3984 (1996).
 - [14] Reciprocal Lattice Unit (r.l.u.)
 - [15] The depletion of the incident beam due to scattering by various crystallites (secondary extinction).
 - [16] F. Jona and G. Shirane: Ferroelectric crystals, Dover ed. (Pergamon Press, Oxford, 1992) p. 161.
 - [17] The crystal lattice of the M_A phase is defined as $a_{M_A} = a_c + b_c$, $b_{M_A} = a_c - b_c$ and $c_{M_A} = c_c$, where a_c , b_c and c_c are unit vectors of a cubic lattice.
 - [18] In Fig. 7(b), the angle of each monoclinic phase is related to the real monoclinic angle β_{M_A} and β_{M_C} as $\tan \beta = 2 \tan \beta_{M_A}$ and $\beta = \beta_{M_C}$.
 - [19] Omega scan is one which goes perpendicularly to the in-plane scattering vector.
 - [20] Y. Yamada and Y. Uesu, Solid State Commun. 81, 777 (1992).
 - [21] K. Hirota, Z.G. Ye, S. Wakimoto, P.M. Gehring and G. Shirane, Phys. Rev. B 65, 104105 (2002).
 - [22] Y. Uesu, M. Matsuda, Y. Yamada, K. Fujishiro, D. E. Cox, B. Noheda and G. Shirane, J. Phys. Soc. Jpn. 71, 960 (2002).
 - [23] G. Xu et al., private communication.